Quantum Electrodynamics and Quantum Optics: Lecture 4

Fall 2025

Ill. Niklas Elmehed © Nobel Prize Outreach

John Clarke

Prize share: 1/3

Ill. Niklas Elmehed © Nobel Prize Outreach

Michel H. Devoret

Prize share: 1/3

Ill. Niklas Elmehed © Nobel Prize Outreach

John M. Martinis

Prize share: 1/3

The Nobel Prize in Physics 2025 was awarded jointly to John Clarke, Michel H. Devoret and John M. Martinis "for the discovery of macroscopic quantum mechanical tunnelling and energy quantisation in an electric circuit"

Measurements of Macroscopic Quantum Tunneling out of the Zero-Voltage State of a Current-Biased Josephson Junction

Michel H. Devoret,[a] John M. Martinis, and John Clarke
Department of Physics, University of California, Berkeley, California 94720, and Materials and Molecular Research Division, Lawrence Berkeley Laboratory, Berkeley, California 94720
(Received 26 July 1985)

The escape rate of an underdamped ($Q \approx 30$), current-biased Josephson junction from the zero-voltage state has been measured. The relevant parameters of the junction were determined *in situ* in the thermal regime from the dependence of the escape rate on bias current and from resonant activation in the presence of microwaves. At low temperatures, the escape rate became independent of temperature with a value that, with no adjustable parameters, was in excellent agreement with the zero-temperature prediction for macroscopic quantum tunneling.

PACS numbers: 74.50.+r, 03.65.−w, 05.30.−d, 05.40.+j

Quantum Mechanics of a Macroscopic Variable: The Phase Difference of a Josephson Junction

John Clarke, Andrew N. Cleland, Michel H. Devoret, Daniel Esteve, John M. Martinis

Experiments to investigate the quantum behavior of a macroscopic degree of freedom, namely the phase difference across a Josephson tunnel junction, are described. The experiments involve measurements of the escape rate of the junction from its zero voltage state. Low temperature measurements of the escape rate for junctions that are either nearly undamped or moderately damped agree very closely with predictions for macroscopic quantum tunneling, with no adjustable parameters. Microwave spectroscopy reveals quantized energy levels in the potential well of the junction in excellent agreement with quantum-mechanical calculations. The system can be regarded as a "macroscopic nucleus with wires."

emphasized, one must distinguish carefully between macroscopic quantum phenomena originating in the superposition of a large number of microscopic variables and those displayed by a single macroscopic degree of freedom. It is the latter that we discuss in this article.

Our usual observations on a billiard ball or Brownian particle reveal classical behavior because Planck's constant $\hbar$ is so tiny. However, at least in principle there is nothing to prevent us from designing an experiment in which these objects are quantum mechanical. To do so we have to satisfy two criteria: (i) the thermal energy must be small compared with the separation of the quantized energy levels, and (ii) the macroscopic degree of freedom must be sufficiently decoupled from all other degrees of freedom if the lifetime of the quantum states is to be longer than the characteristic time scale of the system (*1*). To illustrate the application of these

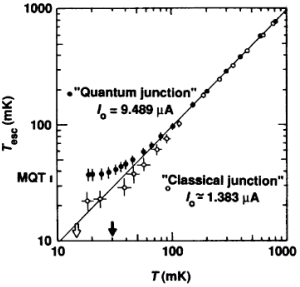

Fig. 4. T_{esc} versus T at $\ell n(\omega_p/2\pi\Gamma) = 11$ for the high and low values of I_0 with arrows indicating T_{cr} (solid and open circles and arrows). The vertical bar labeled MQT is the prediction for $I_0 = 9.489$ μA. The line is the thermal prediction $T_{esc} = 0.95T$. Horizontal error bars are a combination of systematic and random errors in the temperature scale; vertical error bars indicate primarily systematic uncertainties in the junction parameters. For clarity, error bars for T have been shown for the "classical junction" only; identical errors apply to the "quantum junction."

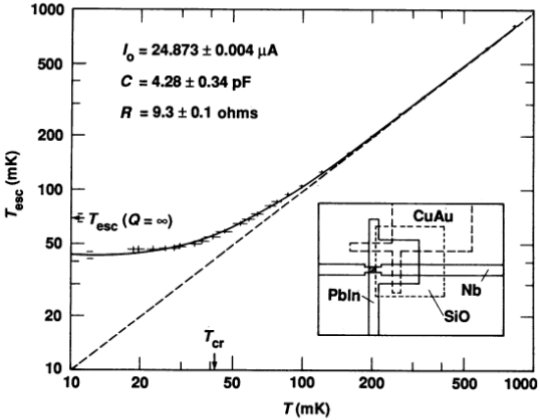

Fig. 5. T_{esc} versus T for shunted junction (configuration shown in inset). Solid curve is theory, dashed line is classical prediction $T_{esc} = 0.98T$. The crossover temperature T_{cr} for this junction and T_{esc} for $Q = \infty$ are indicated by arrows. Error bars are as in Fig. 4.

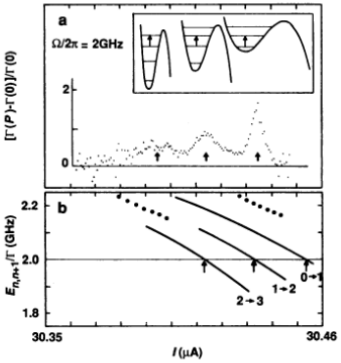

Fig. 6. (**a**) $[\Gamma(P) - \Gamma(0)]/\Gamma(0)$ versus I for an 80 by 10 μm^2 junction at 28 mK in the presence of 2.0 GHz microwaves ($k_B T/\hbar\Omega = 0.29$). Arrows indicate values of current at which the peaks of the resonances occur. Inset represents the corresponding transitions between energy levels. (**b**) Calculated energy-level spacings $E_{n,n+1}$ versus I for $I_0 = 30.572 \pm 0.017$ μA and $C = 47.0 \pm 3.0$ pF. Dotted lines indicate uncertainties in the $0 \rightarrow 1$ curve that arise from uncertainties in I_0 and C. Arrows indicate values of bias current at which resonances are predicted to occur.

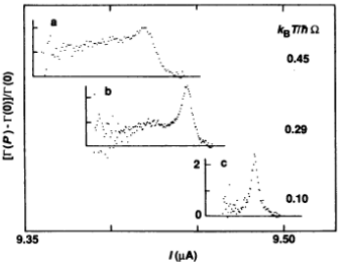

Fig. 7. $[\Gamma(P) - \Gamma(0)]/\Gamma(0)$ versus I for a 10 by 10 μm^2 junction with $I_0 \approx 9.57$ μA and $C \approx 6.35$ pF at three values of $k_B T/\hbar\Omega$. The microwave frequencies are: curve a, 4.5 GHz; curve b, 4.1 GHz; and curve c, 3.7 GHz.

P-Function[1]

P-function

We introduce the P-function or the Glauber-Sudarshan phase space representation $P(\alpha)$ as

$$\rho = \int P(\alpha) \left|\alpha\right\rangle \left\langle\alpha\right| \mathrm{d}^2\alpha.$$

The P-function has the following properties:

$$\int \mathrm{d}^2\alpha P(\alpha) = 1 \quad P^*(\alpha) = P(\alpha).$$

It is often used to compute the expectations of a normally ordered function:

$$\left\langle \hat{a}^{\dagger m}\hat{a}^n \right\rangle = \mathrm{Tr}(\hat{a}^n\rho\hat{a}^{\dagger m}) = \int \mathrm{d}^2\alpha P(\alpha)\alpha^{*m}\alpha^n$$

where $P(\alpha)$ is a quasi-probability function which diagonalizes the density operator in the coherent state basis.

[1] Glauber, R. J. (1963). Coherent and incoherent states of the radiation field. Physical Review, 131(6), 2766.

P-Function

- Coherent states $\rho = |\alpha_0\rangle\langle\alpha_0|$: $P(\alpha) = \delta(\alpha - \alpha_0)$

$$\text{Variance:} \quad \left\langle \Delta\hat{n}^2 \right\rangle = \left\langle (\hat{a}^\dagger\hat{a})^2 - \left\langle \hat{a}^\dagger\hat{a} \right\rangle^2 \right\rangle = \left\langle \hat{a}^{\dagger 2}\hat{a}^2 + \hat{a}^\dagger\hat{a} - \left\langle \hat{a}^\dagger\hat{a} \right\rangle^2 \right\rangle \quad \text{normal order}$$

$$= \int \mathrm{d}^2\alpha \underbrace{P(\alpha)}_{\delta(\alpha-\alpha_0)} (|\alpha|^4 + |\alpha|^2) - \left[\int \mathrm{d}^2\beta \underbrace{P(\beta)}_{\delta(\beta-\alpha_0)} |\beta|^2 \right]^2$$

$$= |\alpha_0|^2$$

- Fock states $\rho = |n\rangle\langle n|$: $P(\alpha) = \frac{e^{|\alpha|^2}}{n!} \frac{\partial^{2n}}{\partial\alpha^n \partial\alpha^{*n}} \delta^{(2)}(\alpha)$, where $\delta^{(2)}(\alpha) = \delta(\alpha)\delta(\alpha^*)$ and δ the complex Dirac function.
- Also worth noting the operator correspondences:[2] $\hat{a}^\dagger |\alpha\rangle\langle\alpha| = (\alpha^* + \frac{\partial}{\partial\alpha}) |\alpha\rangle\langle\alpha|$ and $|\alpha\rangle\langle\alpha| \hat{a} = (\alpha + \frac{\partial}{\partial\alpha^*}) |\alpha\rangle\langle\alpha|$.

[2] Scully, M.O., Zubairy, M.S. "Quantum optics" (1999). Page 79

Can a $P(\alpha, \alpha^*)$ be found for every density matrix?

The Characteristic Function of the P representation[3]

$$\chi_N(z, z^*) \equiv \mathbf{Tr}[\rho e^{iz^* a^\dagger} e^{iza}] = \int P(\alpha, \alpha^*) e^{iz^*\alpha^*} e^{iz\alpha} \mathrm{d}^2\alpha$$

P function expressed in the Fock state basis

$$P(\alpha, \alpha^*) = \int \mathrm{d}^2 z \sum_{n,m,k} \rho_{n+k,m+k} \sqrt{(n+k)!(m+k)!} (iz^*)^m (iz)^n e^{-iz^*\alpha^*} e^{iz\alpha} / k!m!n!$$

Normal ordered operator products

$$\langle (\hat{a}^\dagger)^p (\hat{a})^q \rangle = \frac{\partial^{p+q}}{\partial (iz^*)^p \partial (iz)^q} \chi_N(z, z^*)|_{z=z^*=0}$$

[3] Carmichael, H. J. (1999). Statistical Methods in Quantum Optics 1. Springer., pages 84 & 95

Historical link to Wigner function

- **E. P. Wigner (1932)[4]:** introduced the Wigner function to study quantum corrections to classical statistical mechanics.
- **Ville (1948)[5]:** adapted Wigner's construction to signal analysis, leading to the Wigner–Ville distribution.

On the Quantum Correction For Thermodynamic Equilibrium

By E. WIGNER
Department of Physics, Princeton University
(Received March 14, 1932)

The probability of a configuration is given in classical theory by the Boltzmann formula $\exp[-V/hT]$ where V is the potential energy of this configuration. For high temperatures this of course also holds in quantum theory. For lower temperatures, however, a correction term has to be introduced, which can be developed into a power series of h. The formula is developed for this correction by means of a probability function and the result discussed.

[4] E. P. Wigner (1932). "On the quantum correction for thermodynamic equilibrium". Physical Review. 40 (5): 749–759.

[5] J. Ville, "Théorie et Applications de la Notion de Signal Analytique", Câbles et Transmission, 2, 61–74 (1948)

Wigner function and the time-frequency distribution[6]

Time-frequency distribution

From standard Fourier analysis, recall that the instantaneous energy of a signal $s(t)$ is the absolute value of the signal squared:

$$|s(t)|^2 = \text{intensity per unit time at time } t$$

The intensity per unit frequency, the energy density spectrum, is the absolute value of the Fourier transform squared,

$$|S(\omega)|^2 = \text{intensity per unit frequency at } \omega$$

They are related to each other by Fourier transform:

$$S(\omega) = \frac{1}{\sqrt{2\pi}} \int s(t) e^{-i\omega t} dt$$

[6] Cohen, "Time-frequency distribution - A review", Proceedings of the IEEE, vol. 77, no. 7, pp. 941-981, July 1989

Wigner function and the time-frequency distribution[7]

Time-frequency distribution

The fundamental goal is to devise a joint function of time and frequency that represents the intensity per unit time per unit frequency:

$$P(t,\omega) = \text{intensity at time } t \text{ and frequency } \omega$$

satisfying the marginal properties:

$$\int P(t,\omega)\,dt = |S(\omega)|^2, \qquad \int P(t,\omega)\,d\omega = |s(t)|^2,$$

and the total energy:

$$E = \int P(t,\omega)\,dt\,d\omega.$$

[7] Cohen, "Time-frequency distributions — A review," *Proceedings of the IEEE*, vol. 77, no. 7, pp. 941–981, July 1989.

Wigner function and the time-frequency distribution[8]

Ville derived a distribution that Wigner gave in 1932 to study quantum statistical mechanics.

Wigner-Ville distribution

$$W(t,\omega) = \frac{1}{2\pi}\int s^*(t-\frac{1}{2}\tau)e^{-i\tau\omega}s(t+\frac{1}{2}\tau)d\tau$$

Properties

$$\int W(t,\omega)dt = |S(\omega)|^2, \ \int W(t,\omega)d\omega = |s(t)|^2$$

$$E = \int W(t,\omega)dtd\omega$$

[8] Cohen, "Time-frequency distribution - A review", Proceedings of the IEEE, vol. 77, no. 7, pp. 941-981, July 1989

Wigner-Ville distribution for a sine wave with changed frequency[9]

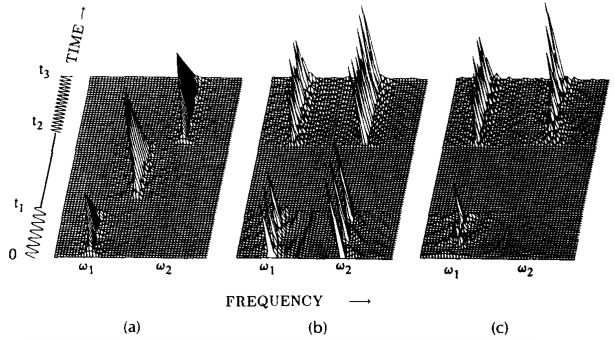

Figure: (a) Wigner, (b) Rihaczek, and (c) Page distributions for the signal illustrated at left. The signal is turned on at time zero with constant frequency ω_1, and turned off at time t_1, turned on again at time t_2,with frequency ω_2,and turned off at time t_3.All three distributions display energy density where one does not expect any. The positive parts of the distributions are plotted. For the Rihaczek distribution we have plotted the real part, which is also a distribution.

[9] Cohen, "Time-frequency distribution - A review", Proceedings of the IEEE, vol. 77, no. 7, pp. 941-981, July 1989

Wigner-Ville distribution for a sine wave with changed frequency[10]

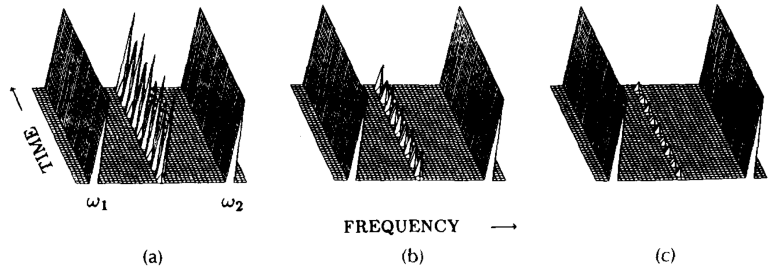

Figure: (a)Wigner and (b), (c) Choi-Williams distributions for the sum of two sine waves, $s(t) = e^{i\omega_1 t} + e^{i\omega_2 t}$.The Wigner distribution is peaked to infinity at the frequencies ω_1, ω_2 and at the spurious value of $\omega = 1/2(\omega_1 + \omega_2)$.The middle term oscillatesand is due to the cross terms. The Choi-Williams distributions are shown for (b) $\sigma = 10^6$ and (c) $\sigma = 10^5$. Note that all three distributions satisfy the marginals.The values for ω are $\omega_1 = 1$ and $\omega_2 = 9$. The delta functions at ω_1, ω_2 are symbolically represented and are cut off at the value of 700.

[10] Cohen, "Time-frequency distribution - A review", Proceedings of the IEEE, vol. 77, no. 7, pp. 941-981, July 1989

Wigner-Ville distribution for a chirped pulse[11]

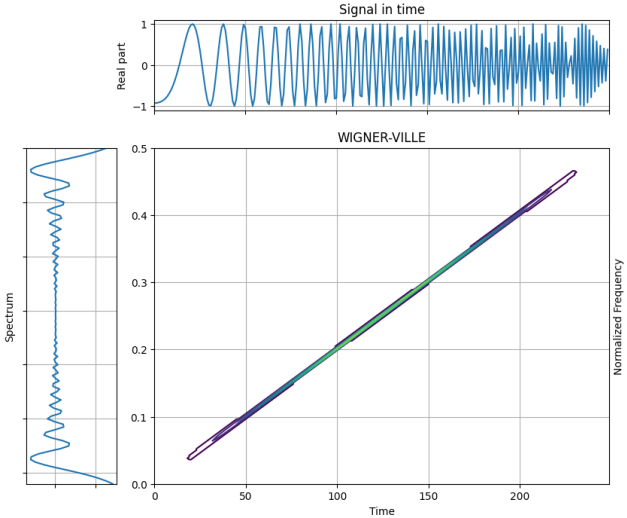

[11] PyTFTB, https://tftb.readthedocs.io

Relationship Between Quantum Mechanics and Signal Analysis[12]

Quantum Mechanics (Inherently Probabilistic)		Signal Analysis (Deterministic)	
Position	q (random)	Time	t
Momentum	p (random)	Frequency	ω
Time	t	No correspondence	
Wave function	$\psi(q,\, t)$	Signal	$s(t)$
Momentum wave function	$\phi(p,\, t) = \frac{1}{\sqrt{2\pi\hbar}} \int \psi(q,\, t)\, e^{-jqp/\hbar}\, dq$	Spectrum	$S(\omega) = \frac{1}{\sqrt{2\pi}} \int s(t)\, e^{-j\omega t}\, dt$
Probability of position at time t	$\lvert\psi(q,\, t)\rvert^2$	Energy density	$\lvert s(t)\rvert^2$
Probability of momentum at time t	$\lvert\phi(p,\, t)\rvert^2$	Energy density spectrum	$\lvert S(\omega)\rvert^2$
Expected value of position	$\langle q\rangle = \int q\lvert\psi(q,\, t)\rvert^2\, dq$	Mean time	$\langle t\rangle = \int t\lvert s(t)\rvert^2\, dt$
Expected value of momentum	$\langle p\rangle = \int p\lvert\phi(p,\, t)\rvert^2\, dp$	Mean frequency	$\langle\omega\rangle = \int \omega\lvert S(\omega)\rvert^2\, d\omega$
Standard deviation of position	$\sigma_q = \sqrt{\langle q^2\rangle - \langle q\rangle^2}$	Duration	$T = \sqrt{\langle t^2\rangle - \langle t\rangle^2}$
Standard deviation of momentum	$\sigma_p = \sqrt{\langle p^2\rangle - \langle p\rangle^2}$	Bandwidth	$B = \sqrt{\langle\omega^2\rangle - \langle\omega\rangle^2}$
Uncertainty principle	$\sigma_p\sigma_q \geq \hbar/2$	Time-bandwidth relation	$BT \geq \frac{1}{2}$

*The formal mathematical correspondence is (position, momentum) $\Leftrightarrow$ (time, frequency). The wave function in quantum mechanics depends on time, but this has no formal correspondence in signal analysis. Planck's constant $\hbar$ may be taken equal to 1. Quantum mechanics is an inherently probabilistic theory in contrast to signal analysis, which is deterministic. Hence while there is the formal mathematical correspondence, the interpretation of results is very different. Both quantum mechanics and signal theory have another level of indeterminism where the wave function or the signal is ensemble averaged.

[12] Cohen, "Time-frequency distribution - A review", Proceedings of the IEEE, vol. 77, no. 7, pp. 941-981, July 1989

Wigner function

Definition

$$W(p,q) = \frac{1}{2\pi}\int_{-\infty}^{\infty} \exp(ipx)\left\langle q - \frac{x}{2}\right|\hat{\rho}\left|q + \frac{x}{2}\right\rangle dx$$

Marginal distributions

$$\langle p|\,\rho\,|p\rangle = |\psi(p)|^2 = \int_{-\infty}^{\infty} W(p,q)dq \qquad \langle q|\,\rho\,|q\rangle = |\psi(q)|^2 = \int_{-\infty}^{\infty} W(p,q)dp$$

Basic Properties

- Real $W^*(q,p) = W(q,p)$
- $\mathbf{Tr}[\hat{\rho}_1\hat{\rho}_2] = 2\pi\int\int W_1(q,p)W_2(q,p)dqdp$ or $|\,\langle\Psi_1|\Psi_2\rangle\,|^2 = 2\pi\int\int W_1(q,p)W_2(q,p)dqdp$
- $\mathbf{Tr}[\hat{\rho}^2] = \int 2\pi W(q,p)^2 dqdp \leq 1$

From classical statistics to quantum phase space

In classical statistical mechanics, the state of a particle is described by a joint probability density $f(q,p)$ in phase space. In quantum mechanics, the Heisenberg uncertainty principle forbids simultaneous precise knowledge of position and momentum. Nevertheless, Wigner (1932) introduced a quasi-probability distribution $W(q,p)$ that extends the classical concept of a phase-space density while preserving correct marginal properties.

Postulate defining the Wigner function

The probability distribution of the rotated quadrature q_θ is obtained as the marginal of the Wigner function:

$$\Pr(q_\theta,\theta) = \int_{-\infty}^{\infty} W(q_\theta\cos\theta - p_\theta\sin\theta, q_\theta\sin\theta + p_\theta\cos\theta)dp_\theta.$$

This relation uniquely defines the Wigner function $W(q,p)$ with experimentally measurable quadrature histograms in optical homodyne tomography.

Wigner Function[13]

Wigner function, the phase-space quasi-probability density

$$W_{\hat{\rho}}(q,p) = \frac{1}{2\pi}\int_{-\infty}^{\infty}\left\langle q+\frac{1}{2}q'\right|\hat{\rho}\left|q-\frac{1}{2}q'\right\rangle e^{-ipq'}dq'$$

$$\Pr(q_\theta,\theta) = \int_{-\infty}^{\infty} W(q_\theta\cos\theta - p_\theta\sin\theta, q_\theta\sin\theta + p_\theta\cos\theta)dp_\theta.$$

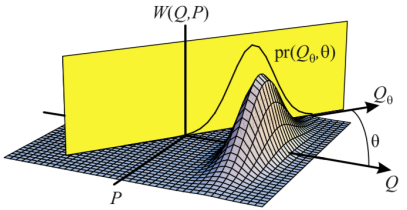

The experimentally measured probability density $\Pr(q_\theta,\theta)$ is the integral projection of the Wigner function $W_{\hat{\rho}}(q,p)$ onto a vertical plane defined by the phase of the local oscillator.

[13] Lvovsky, Alexander I., and Michael G. Raymer. "Continuous-variable optical quantum-state tomography." *Reviews of Modern Physics* 81.1 (2009): 299.

Wigner function

Coherent state

$$\alpha = \frac{1}{2}(X_1 + iX_2), \qquad X_i = \langle \hat{x}_i \rangle$$

$$\langle (\Delta \hat{x}_1)^2 \rangle = \langle (\Delta \hat{x}_2)^2 \rangle = 1$$

$$W(x_1', x_2') = \frac{2}{\pi} e^{-\frac{1}{2}(x_1'^2 + x_2'^2)}, \qquad x_i' = x_i - X_i$$

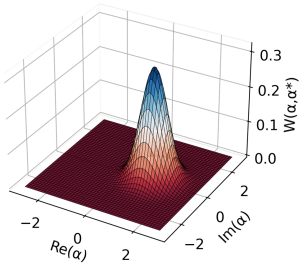

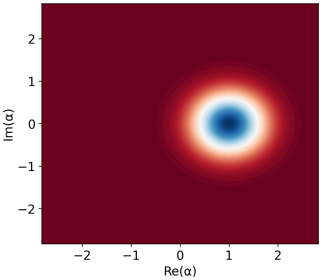

Wigner function

Squeezed state

$$W(x_1', x_2') = \frac{2}{\pi} e^{-\frac{1}{2}(x_1'^2 e^{-2r} + x_2'^2 e^{+2r})}$$

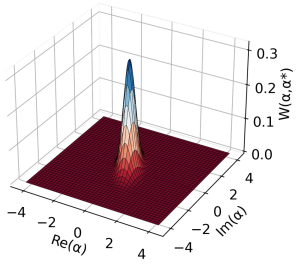

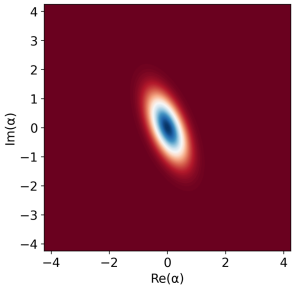

Wigner function

Fock state

For the state $|1\rangle$: $\quad W(\alpha, \alpha^*) = \frac{2}{\pi} e^{-2|\alpha|^2}(4|\alpha|^2 - 1)$

Negative at the origin.

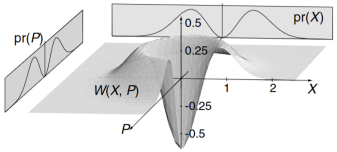

FIG. 1. Theoretical phase space quasiprobability density (Wigner function) of the single-photon state $|1\rangle$: $W(X,P) = \frac{2}{\pi}[4(X^2+P^2)-1]e^{-2(X^2+P^2)}$. $\hat{X} = (\hat{a} + \hat{a}^\dagger)/\sqrt{2}$ and $\hat{P} = (\hat{a} - \hat{a}^\dagger)/\sqrt{2}i$ are normalized noncommuting electric field quadrature observables. Single-quadrature probability densities (*marginal distributions*) are also displayed.

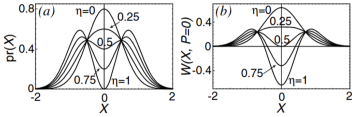

FIG. 3. Effect of the nonperfect measurement efficiency η on the marginal distribution (a) and the reconstructed WF (b). For the WF, cross sections by the plane $P = 0$ are shown. Negative values require $\eta > 0.5$.

[13] Lvovsky, Alexander I., et al. "Quantum state reconstruction of the single-photon Fock state." Physical Review Letters 87.5 (2001): 050402.

Influence of a beamsplitter splitting ratio on Wigner function measurement

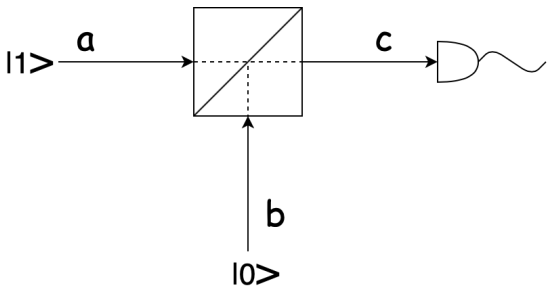

$$\hat{c} = \sqrt{\eta}\hat{a} + i\sqrt{1-\eta}\hat{b}$$

If we measure the Wigner function at port c, with η larger than 0.5, the negativity of the Wigner function is observable.

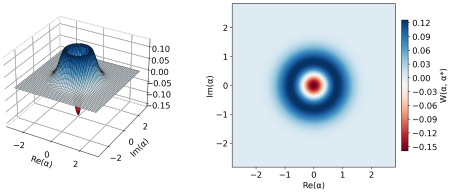

Figure: $\eta = 0.75$

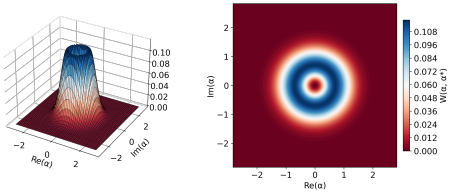

Figure: $\eta = 0.5$

Wigner function

Symmetric Characteristic Function

$$\chi_s \equiv \mathbf{Tr}[\rho e^{\beta a^\dagger - \beta^* a}] \equiv \mathbf{Tr}[\rho D(\beta)]$$

$$W(\alpha, \alpha^*) \equiv \frac{1}{\pi^2} \int \chi_s(\beta, \beta^*) e^{-\beta\alpha^*} e^{\beta^*\alpha} \mathrm{d}^2\beta$$

$$\left\langle \frac{a^\dagger a + a a^\dagger}{2} \right\rangle = \int W(\alpha)\, \alpha^* \alpha \, \mathrm{d}^2\alpha$$

Calculation of Wigner Function

If $\rho = |\phi\rangle \langle\phi|$, then

$$\boxed{W_\phi(\alpha, \alpha^*) = \frac{1}{\pi^2} \int \mathrm{d}^2 z \; e^{\beta^*\alpha - \beta\alpha^*} \; \langle\phi| \; D(\beta) \; |\phi\rangle}$$

Examples for calculation of Wigner function

Fock State

For a Fock state $|n\rangle$,

$$\langle n|\, D(\beta)\, |n\rangle = e^{-\frac{1}{2}|\beta|^2} \sum_{m=0}^{n} \frac{(-|\beta|^2)^m}{m!} \binom{n}{m} = e^{-\frac{1}{2}|\beta|^2} L_n(|\beta|^2),$$

where $L_n(x)$ is the Laguerre polynomial of order n. The corresponding Wigner function is

$$W_n(\alpha) = \frac{2}{\pi}(-1)^n e^{-2|\alpha|^2} L_n(4|\alpha|^2).$$

$L_1(x) = 1 - x$, we have

$$W_1(\alpha) = \frac{2}{\pi}(-1)\, e^{-2|\alpha|^2}\, L_1(4|\alpha|^2) = \frac{2}{\pi}\, e^{-2|\alpha|^2}\, (4|\alpha|^2 - 1).$$

Examples for calculation of Wigner function

Squeezed Vacuum State

For a squeezed vacuum $|\xi\rangle = \hat{S}(\xi)\,|0\rangle$, using $\hat{S}^\dagger(\xi) D(\beta) \hat{S}(\xi) = D(\beta\mu + \beta^* \nu)$ with $\mu = \cosh|\xi|$ and $\nu = e^{i\varphi_\nu} \sinh|\xi|$, we have

$$W(\alpha) = \frac{1}{\pi^2} \int \mathrm{d}^2\beta \; e^{\alpha\beta^* - \alpha^*\beta} e^{-\frac{1}{2}|\beta\mu + \beta^*\nu|^2}.$$

For real squeezing parameter $\xi \in \mathbb{R}$, the integration gives

$$W(\alpha) = \frac{2}{\pi} \exp\left[-2 \left(\frac{(\mathrm{Re}\,\alpha)^2}{e^{-2\xi}} + \frac{(\mathrm{Im}\,\alpha)^2}{e^{2\xi}} \right) \right].$$

Quantum state tomography

Motivation

To reconstruct a quantum state of light, we cannot directly measure ρ_{nn} with a photo-detector but we can measure $\Pr(X_\theta)$ and reconstruct the full Wigner function.

$$X_\theta = \langle X_\theta | \rho | X_\theta \rangle = \langle X | U_\theta^\dagger \rho U_\theta | X \rangle$$

$$\Pr(X_\theta) = \int_{-\infty}^{\infty} W(p_\theta, q_\theta) dp_\theta$$

$$W_\theta(r) = -\frac{1}{\pi} \int_r^\infty \Pr(X_\theta)(X_\theta^2 - r^2)^{-1/2} dX_\theta$$

It is only posible to obtain such $W_\theta(r)$ when the Wigner function is rotationally symmetric[14]

[14] Vogel, W., Welsch, D.G. "Quantum Optics" (2001). Chapter 7

State Reconstruction

Inverse Radon transformation

$$W_{\text{det}}(q,p) = \frac{1}{2\pi^2}\int_0^{\pi}\int_{-\infty}^{\infty} \Pr(q_\theta,\theta) \times K(q\cos\theta + p\sin\theta - q_\theta) dq_\theta d\theta$$

with the integration kernel $K(x) = \frac{1}{2}\int_{-\infty}^{\infty} |\xi| e^{i\xi x} d\xi$. The density matrix can then be reconstructed using the pattern function method.

Maximum likelihood reconstruction

$$L = \Pi_i \Pr_{\hat{\rho}}(q_i,\theta_i)$$

is the likelihood function given the measured data set $\{(q_i,\theta_i)\}$ where $\hat{\rho}$ is the density matrix to be optimized.

Quantum Toolbox

Papers Using QuTiP

56. **Molony** et al., "Creation of Ultracold ^{87}RbCs Molecules in the Rovibrational Ground State", Phys. Rev. Lett. **113**, 255301 (2014).

55. **Lecocq** et al., "Resolving the vacuum fluctuations of an optomechanical system using an artificial atom", Nat. Phys. **11**, 635 (2015).

54. **Bassereh** et al., "Effect of Noise on the Efficiency of Quantum Excitation Energy Transfer In a Toy Model of a Linear Protein Structure", arXiv:1408.6256

53. **Müller** et al., "Coherent Generation of Nonclassical Light on Chip via Detuned Photon Blockade", Phys. Rev. Lett. **114**, 233601 (2015).

52. **Reimann** et al., "Cavity-Modified Collective Rayleigh Scattering of Two Atoms", Phys. Rev. Lett. **114**, 023601 (2015).

51. **Ostermann** et al., "Protected subspace Ramsey metrology", Phys. Rev. A **90**, 053823 (2014).

50. **Mari** et al., "Quantum optomechanical piston engines powered by heat", J. Phys. B **48**, 175501 (2015).

49. **Lin** et al., "Josephson parametric phase-locked oscillator and its application to dispersive readout of superconducting qubits", Nat. Commun. **5**, 4480 (2014).

48. **Lagoudakis** et al., "Hole Spin Pumping and Re-pumping in a p-type δ-doped InAs Quantum Dot", Phys. Rev. B **90**, 121402(R) (2014).

47. **Figueiredo Roque** et al., "Dissipation-driven squeezed and sub-Poissonian mechanical states in quadratic optomechanical systems", arXiv:1406.1987

Quantum Toolbox

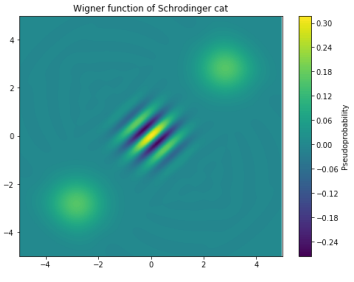

Wigner function of cat states

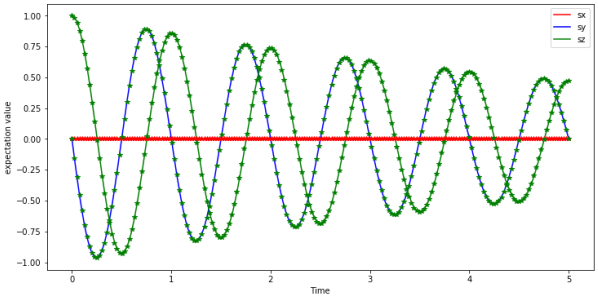

Time evolution of a qubit

Literature review

Measurement of the quantum states of squeezed light

G. Breitenbach, S. Schiller & J. Mlynek

Fakultät für Physik, Universität Konstanz, D-78457 Konstanz, Germany

A state of a quantum-mechanical system is completely described by a density matrix or a phase-space distribution such as the Wigner function. The complete family of squeezed states of light (states that have less uncertainty in one observable than does the vacuum state) have been generated using an optical parametric amplifier, and their density matrices and Wigner functions have been reconstructed from measurements of the quantum statistics of their electric fields.

Literature review

The relation between the measured distributions and the density operator ρ is $P_\theta(x_\theta) = \langle x \mid U^\dagger(\theta)\rho U(\theta) \mid x \rangle$, where $U(\theta) = \exp(-i\theta a^\dagger a)$ performs a rotation in phase space. As the optical state evolves freely with ω, U is equivalent to the time evolution operator with $\theta = \omega t +$ constant, and the θ-dependence of P_θ is equivalent to the time dependence of the position probability density of the state (that is, of $|\psi(x,t)|^2$, if $\rho = |\psi\rangle\langle\psi|$ is a pure state). Thus, homodyne detection maps out the time evolution of a harmonic oscillator state. Our measurements (shown below) may be regarded as an implementation of the oldest example of quantum dynamics, the motion of a wavepacket in a harmonic potential studied by Schrödinger in 1926[23].

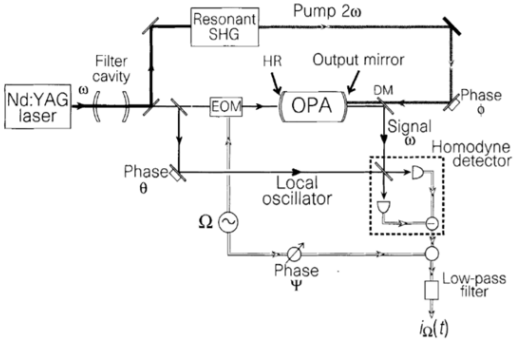

Figure 1 Experimental scheme for generating bright squeezed light and squeezed vacuum with an optical parametric oscillator (OPA). The electric field quadratures are measured in the homodyne detector while scanning the phase θ. A computer performs the statistical analysis of the photocurrent i_Ω and reconstructs the quantum states. EOM, electro-optic modulator; DM, dichroic mirror; SHG, second harmonic generator; HR, high reflector.

Literature review

Of the various methods that have been proposed to reconstruct the quantum state numerically from the set of measured distributions P_θ, two are employed here. The first method makes use of the fact that the distributions $P_\theta(x_\theta)$ are the marginals of the Wigner function $W(x, y)$ in rotated coordinates;

$$P_\theta(x_\theta) = \int_{-\infty}^{\infty} W(x_\theta \cos\theta - y_\theta \sin\theta, x_\theta \sin\theta + y_\theta \cos\theta)\, \mathrm{d}y_\theta \qquad (1)$$

where $y_\theta = -x \sin\theta + y \cos\theta$. Therefore $W(x, y)$ can be obtained from the set P_θ by back-projection via the inverse Radon transform[2]. The second method furnishes the elements of the density matrix in the Fock basis via integration of the distributions P_θ over a set of pattern functions[3,4]. In contrast to the inverse Radon transform, this procedure does not involve any filtering of the experimental data and also allows an estimation of the propagation of statistical errors.

Literature review

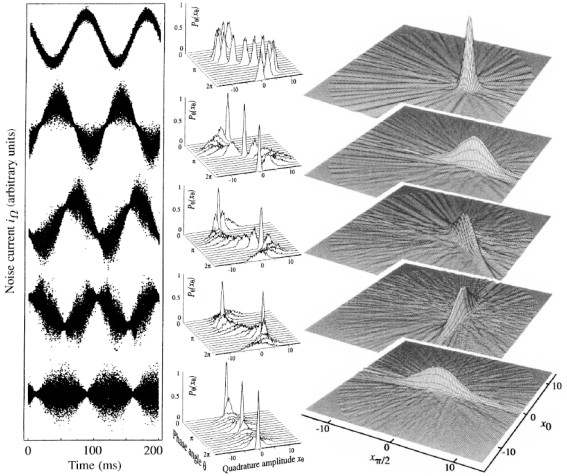

Figure 2 Noise traces in $i_D(t)$ (left), quadrature distributions $P_\phi(x_\phi)$ (centre), and reconstructed Wigner functions (right) of generated quantum states. From the top: Coherent state, phase-squeezed state, state squeezed in the $\phi = 48°$-quadrature, amplitude-squeezed state, squeezed vacuum state. The noise traces as a function of time show the electric fields' oscillation in a 4π interval for the upper four states, whereas for the squeezed vacuum (belonging to a different set of measurements) a 3π interval is shown. The quadrature distributions (centre) can be interpreted as the time evolution of wave packets (position probability densities) during one oscillation period. For the reconstruction of the quantum states a π interval suffices.

Review of the paper presentation this week

VOLUME 59, NUMBER 18 PHYSICAL REVIEW LETTERS 2 NOVEMBER 1987

Measurement of Subpicosecond Time Intervals between Two Photons by Interference

C. K. Hong, Z. Y. Ou, and L. Mandel
Department of Physics and Astronomy, University of Rochester, Rochester, New York 14627
(Received 10 July 1987)

A fourth-order interference technique has been used to measure the time intervals between two photons, and by implication the length of the photon wave packet, produced in the process of parametric down-conversion. The width of the time-interval distribution, which is largely determined by an interference filter, is found to be about 100 fs, with an accuracy that could, in principle, be less than 1 fs.

PACS numbers: 42.50.Bs, 42.65.Re

Hong–Ou–Mandel effect

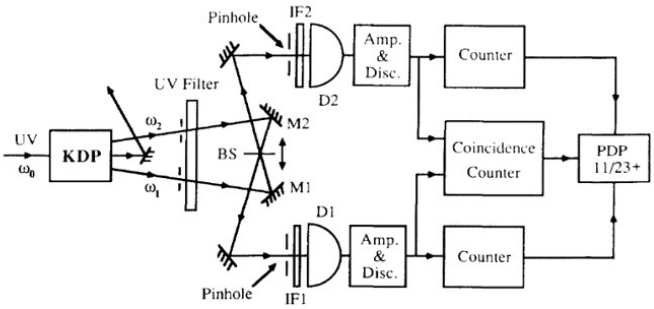

FIG. 1. Outline of the experimental setup.

$$|\psi_{\text{out}}\rangle = (R-T)\,|1_1,1_2\rangle + i(2RT)^{1/2}\,|2_1,0_2\rangle + i(2RT)^{1/2}\,|0_1,2_2\rangle, \tag{2}$$

where R and T are the reflectivity and transmissivity of the beam splitter, with $R+T=1$. It follows that for a 50%:50% beam splitter with $R=\frac{1}{2}=T$, the first term is zero by virtue of the destructive interference of the corresponding two-photon probability amplitudes. No coincidences (other than accidentals) should therefore be registered by detectors D1 and D2.

Hong–Ou–Mandel effect

In practice the down-shifted photons are never monochromatic. Let us represent the two-photon state produced by the potassium-dihydrogen-phosphate crystal by the linear superposition.

$$|\psi\rangle = \int d\omega_1 \, \phi(\omega_1, \omega_0 - \omega_1) \, |\omega_1, \omega_0 - \omega_1\rangle,$$

$$E_1^{(+)}(t) = \sqrt{T} E_{01}^{(+)}(t - \tau_1) + \mathrm{i}\sqrt{R} E_{02}^{(+)}(t - \tau_1 + \delta\tau)$$

$$E_2^{(+)}(t) = \sqrt{T} E_{02}^{(+)}(t - \tau_1) + \mathrm{i}\sqrt{R} E_{01}^{(+)}(t - \tau_1 - \delta\tau)$$

Then the joint probability of the detection of photons at both detectors D1 and D2 at times t and $t + \tau$, respectively, is given by

$$\boxed{P_{12}(\tau) \propto \langle \hat{E}_1^{(-)}(t) \, \hat{E}_2^{(-)}(t+\tau) \, \hat{E}_2^{(+)}(t+\tau) \, \hat{E}_1^{(+)}(t) \rangle.}$$

Hong–Ou–Mandel effect

Given $P_{12}(\tau)$, the number of coincidences measured is $N_c = N_0 - 2RTC\frac{\int_{-\infty}^{\infty} g(\tau)g(\tau-2\delta\tau)d\tau}{\int_{-\infty}^{\infty} g^2(\tau)d\tau}$, with $N_0 = C(R^2+T^2)$.

- $\delta\tau \gg \tau_{\text{corr}}$: at very large delays, autocorrelation vanishes and $N_c = N_0$.
- $\delta\tau \ll \tau_{\text{corr}}$: for minuscule delays, the autocorrelation is perfect and $N_c = C(R-T)^2$.

Model: $\phi(\omega_0/2+\omega, \omega_0/2-\omega)$ - Gaussian with bandwidth $\Delta\omega$. Then $g(\tau)$ is

$$g(\tau) = \exp\left(-\frac{1}{2}(\Delta\omega\tau)^2\right).$$

$$N_c = C(T^2+R^2)\left[1 - \frac{2RT}{R^2+T^2}e^{-(\Delta\omega\,\tau)^2}\right].$$

Hong–Ou–Mandel effect

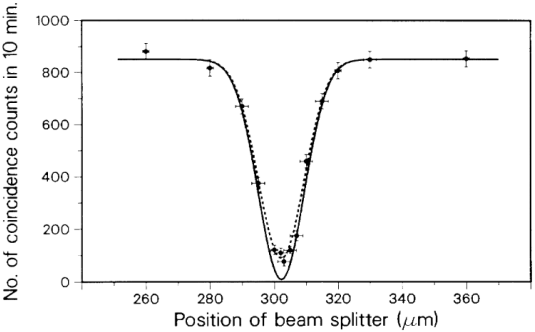

FIG. 2. The measured number of coincidences as a function of beam-splitter displacement $c\,\delta\tau$, superimposed on the solid theoretical curve derived from Eq. (11) with $R/T = 0.95$, $\Delta\omega = 3\times10^{13}$ rad s^{-1}. For the dashed curve the factor $2RT/(R^2+T^2)$ in Eq. (11) was multiplied by 0.9. The vertical error bars correspond to one standard deviation, whereas horizontal error bars are based on estimates of the measurement accuracy.

Paper for next week

Experimental quantum teleportation

Dik Bouwmeester, Jian-Wei Pan, Klaus Mattle, Manfred Eibl, Harald Weinfurter & Anton Zeilinger

Institut für Experimentalphysik, Universität Innsbruck, Technikerstr. 25, A-6020 Innsbruck, Austria

Quantum teleportation—the transmission and reconstruction over arbitrary distances of the state of a quantum system—is demonstrated experimentally. During teleportation, an initial photon which carries the polarization that is to be transferred and one of a pair of entangled photons are subjected to a measurement such that the second photon of the entangled pair acquires the polarization of the initial photon. This latter photon can be arbitrarily far away from the initial one. Quantum teleportation will be a critical ingredient for quantum computation networks.

Paper for next week

VOLUME 87, NUMBER 5 PHYSICAL REVIEW LETTERS 30 JULY 2001

Quantum State Reconstruction of the Single-Photon Fock State

A. I. Lvovsky,* H. Hansen, T. Aichele, O. Benson, J. Mlynek,† and S. Schiller‡
Fachbereich Physik, Universität Konstanz, D-78457 Konstanz, Germany
(Received 14 March 2001; published 11 July 2001)

We have reconstructed the quantum state of optical pulses containing single photons using the method of phase-randomized pulsed optical homodyne tomography. The single-photon Fock state $|1\rangle$ was prepared using conditional measurements on photon pairs born in the process of parametric down-conversion. A probability distribution of the phase-averaged electric field amplitudes with a strongly non-Gaussian shape is obtained with the total detection efficiency of $(55 \pm 1)\%$. The angle-averaged Wigner function reconstructed from this distribution shows a strong dip reaching classically impossible negative values around the origin of the phase space.

DOI: 10.1103/PhysRevLett.87.050402 PACS numbers: 03.65.Wj, 42.50.Dv

Questions for next week

- What's the expression of Wigner function they used
- What measurement data is taken and how is it used to reconstruct the Wigner function
- How does measurement efficiency impact the result
- How does signal-LO mode-matching influence efficiency in homodyne detection
- Why a single laser is used for local-oscillator and signal
- Why do they use a doubler and down-converter for single photon sources
- How does the spatial-temporal pulse shape of single photon match LO
- How is the density matrix reconstructed? What are the values of the off-diagonal terms.